

Cone spline surfaces and spatial arc splines — a sphere geometric approach

Stefan Leopoldseder

*Technische Universität Wien, Institut für Geometrie,
Wiedner Hauptstrasse 8-10, A-1040 Wien, Austria*

Basic sphere geometric principles are used to analyze approximation schemes of developable surfaces with cone spline surfaces, i.e. G^1 -surfaces composed of segments of right circular cones. These approximation schemes are geometrically equivalent to the approximation of spatial curves with G^1 -arc splines, where the arcs are circles in an isotropic metric. Methods for isotropic biarcs and isotropic osculating arc splines are presented that are similar to their Euclidean counterparts. Sphere geometric methods simplify the proof that two sufficiently close osculating cones of a developable surface can be smoothly joined by a right circular cone segment. This theorem is fundamental for the construction of osculating cone spline surfaces. Finally, the analogous theorem for Euclidean osculating circular arc splines is given.

Keywords: Developable surface, cone spline surface, spatial arc spline, circular arc spline, sphere geometry, Laguerre geometry

1 Introduction

Sphere geometry is a classical topic of geometry (see e.g. [2, 14]). But it is also an active area within modern geometry [1, 3] and has been applied to rational PH curves and surfaces and various other problems in computer aided geometric design [16, 17]. In the present paper — which is heavily based on the author's PhD thesis [11] — we use sphere geometry to analyze approximation algorithms of developable surfaces with *cone spline surfaces*, i.e. G^1 -surfaces composed of segments of right circular cones, see for instance the example in Figure 1.

In the CAGD literature, rising attention is given to developable surfaces because they are surfaces that can be unfolded into a plane without stretching or tearing. Thus, there are many industry applications, for instance in sheet-metal and plate-metal based industries. The isometric mapping of a developable surface into the plane needs, in general, numerical computation methods, see e.g. [4, 7, 9, 21]. Redont [18] first uses patches of right circular cones (cones of revolution) as their development and bending into other developable shapes is elementary. Because of the global methods given in [18], the adjustment of a single

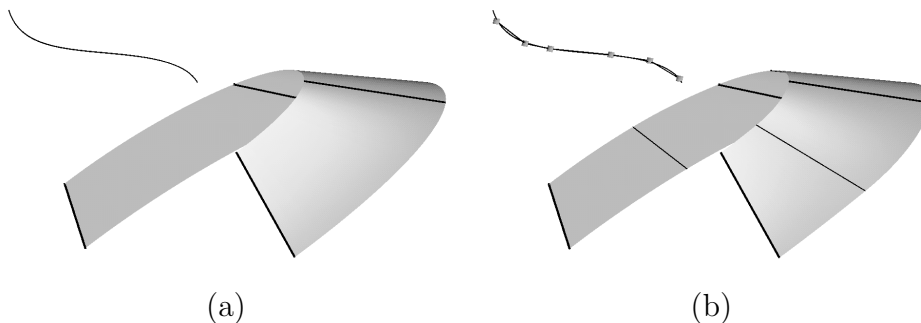


Figure 1: Developable surface (a) and approximating cone spline surface (b)

cone patch affects the position of all adjacent patches. *Local* Hermite approximation schemes based on geometric methods have been presented recently [10, 12].

Developable surfaces are the envelopes of their one parameter set of tangent planes, i.e. they are dual to a spatial curve. For the aim of approximation of developable surfaces we are specially interested in cones of revolution which are special examples of developable surfaces whose tangent planes all touch a one parameter set of spheres. This property motivates using 3-dimensional Euclidean Laguerre geometry in which the elements are *oriented spheres* and *oriented planes* of Euclidean 3-space.

Especially useful for our purposes we will find the so-called isotropic model of this geometry which provides a point representation of oriented planes, thus a curve representation of developable surfaces. Cones of revolution appear as isotropic circles, cone spline surfaces therefore are transformed to spatial isotropic arc splines.

In this paper we will give two curve approximation schemes with spatial isotropic arc splines. The corresponding approximation schemes of developable surfaces with cone spline surfaces can be found in [10]. The first algorithm is an isotropic biarc scheme, whereas the second algorithm constructs an isotropic osculating arc spline of a given spatial curve, i.e. each second of the isotropic arc segments of the arc spline have second order contact with the target curve.

The great advantage of the interpretation of developable surfaces as isotropic curves with the help of Laguerre geometry lies in the fact that curves are easier to handle than surfaces. Thus, we will be able to prove the important theorem that two sufficiently close osculating cones of a developable surface can be smoothly joined by a right circular cone segment. This theorem confirms the feasibility and practicality of the osculating cone spline surface algorithm presented in [10].

Finally, we will prove the Euclidean counterpart of above theorem on isotropic arc splines: Each two, sufficiently close, osculating circles of a twisted curve in Euclidean 3-space can be smoothly joined with a circular arc which gives a G^1 arc spline. Geometric algorithms to construct these Euclidean osculating arc splines

are introduced in [12]. There, a segmentation algorithm of the given spatial curve and approximation errors are given. These investigations also include planar (see also [13]) and spherical osculating arc splines as special cases.

The present paper is structured as follows. Section 2 gives a brief introduction into 3-dimensional Euclidean Laguerre space and its isotropic model. Section 3 describes our first curve approximation scheme, namely with isotropic biarcs. Section 4 provides the second curve approximation scheme producing isotropic osculating arc splines. This section also includes the proof of Theorem 4.1 on the existence of real solution arcs. Finally, section 5 contains the proof of the analogous Theorem 5.1 on Euclidean osculating arcs. It also includes a short introduction to 3-dimensional Euclidean Möbius geometry, another sphere geometry which simplifies our proof.

2 Fundamentals of 3-dimensional Euclidean Laguerre space

For the analytic treatment in real Euclidean 3-space E^3 we will use the affine coordinate vector $\mathbf{x} = (x, y, z)$ to describe a point $\mathbf{x} \in E^3$. Let U denote the set of *oriented planes* \mathbf{u} of E^3 and C the set of *oriented spheres* \mathbf{c} including the points of E^3 as (non-oriented) spheres with radius zero. The elements of C are also called *cycles*. The basic relation between oriented planes and cycles is that of *oriented contact*. An oriented sphere is said to be in oriented contact with an oriented plane if they touch each other in a point and their normal vector in this common point is oriented in the same direction. The oriented contact of a point (nullcycle) and a plane is defined as incidence of point and plane.

Laguerre geometry is the survey of properties that are invariant under the group of so-called *Laguerre transformations* $\alpha = (\alpha_H, \alpha_C)$ which are defined by the two bijective maps

$$\alpha_H : H \rightarrow H, \alpha_C : C \rightarrow C \quad (1)$$

which preserve oriented contact and non-contact between cycles and oriented planes.

Analytically, a plane \mathbf{u} is determined by the equation $u_0 + u_1x + u_2y + u_3z = 0$ with normal vector (u_1, u_2, u_3) . The coefficients u_i are homogeneous plane coordinates $(u_0 : u_1 : u_2 : u_3)$ of \mathbf{u} in the projective extension P^3 of E^3 . Each scalar multiple $(\lambda u_0 : \lambda u_1 : \lambda u_2 : \lambda u_3)$, $\lambda \in \mathbb{R} \setminus \{0\}$ describes the same plane, thus it is possible to use *normalized* homogeneous plane coordinates

$$\mathbf{u} = (u_0 : u_1 : u_2 : u_3), \text{ with } u_1^2 + u_2^2 + u_3^2 = 1 \quad (2)$$

which are appropriate for describing *oriented* planes where the unit normal vector (u_1, u_2, u_3) determines the orientation of the plane.

An oriented sphere (cycle)

$$\mathbf{c} = (x_m, y_m, z_m; r) \quad (3)$$

is determined by its midpoint $\mathbf{m} = (x_m, y_m, z_m)$ and signed radius r . Positive sign of r indicates that the normal vectors are pointing towards the outside of the sphere whereas in the case of negative sign of r they are pointing into the inside. Points of E^3 are cycles characterized by $r = 0$.

The relation of oriented contact is given by

$$u_0 + u_1x_m + u_2y_m + u_3z_m + r = 0 \quad (4)$$

2.1 The isotropic model

As developable surfaces are envelopes of their one parameter family of oriented tangent planes it is appropriate to use a model of Euclidean Laguerre space in which oriented planes are represented by points. Thus, we will briefly discuss the so-called *isotropic model* of Euclidean Laguerre geometry. This model can be obtained by the map

$$\Lambda : U \rightarrow I^3, \quad \Lambda(\mathbf{u}) = \frac{1}{1 - u_3}(u_1, u_2, u_0). \quad (5)$$

which maps oriented hyperplanes $\mathbf{u} \in U$ of E^3 onto points in a 3-dimensional affine space I^3 . u_i denote the normalized homogeneous plane coordinates of \mathbf{u} according to (2). There is a geometric interpretation of the map Λ (see e.g. [11, 17]) which is not essential for the present investigations.

The inverse Λ^{-1} maps each point $\bar{\mathbf{x}} = (\bar{x}, \bar{y}, \bar{z})$ of I^3 to an oriented plane in E^3 with normalized plane coordinates

$$\Lambda^{-1}(\bar{\mathbf{x}}) = \frac{1}{\bar{x}^2 + \bar{y}^2 + 1}(2\bar{z} : 2\bar{x} : 2\bar{y} : \bar{x}^2 + \bar{y}^2 - 1). \quad (6)$$

Formula (5) fails for oriented planes \mathbf{u} with $u_3 = 1$, i.e. normal vector $(0, 0, 1)$. In order to obtain a one-to-one map Λ , one has to extend the point set of I^3 by an affine line of ideal points which correspond to the planes $(u_0 : 0 : 0 : 1)$. Thus one obtains the so-called *isotropic conformal closure* I_M^3 of I^3 . In applications one will apply a suitable coordinate transformation in E^3 such that no planes with normal vector $(0, 0, 1)$ appear. Locally, this is always possible.

By interpreting cycles \mathbf{c} as their set of oriented tangent planes and by applying (5) we obtain

$$\Sigma := \Lambda(\mathbf{c}) : 2\bar{z} + (\bar{x}^2 + \bar{y}^2)(r + z_m) + 2\bar{x}x_m + 2\bar{y}y_m + r - z_m = 0. \quad (7)$$

These surfaces $\Sigma = \Lambda(\mathbf{c})$ are paraboloids of revolution with \bar{z} -parallel axis or, in case of $r + z_m = 0$, planes that are not parallel to the \bar{z} -direction. The \bar{z} -direction is also called *isotropic direction*. The surfaces Σ , defined by (7), are called *isotropic Möbius spheres*. The intersection of two isotropic Möbius spheres is either an ellipse whose top view (normal projection onto $\bar{z} = 0$) is a circle, or a parabola with isotropic axis, or a non-isotropic line. These curves are called *isotropic Möbius circles*.

Let us now look at developable surfaces and cones of revolution, in particular. A developable surface, viewed as envelope of its one parameter family of oriented tangent planes, is mapped to a spatial curve in I^3 via (5). The oriented tangent planes of a cone of revolution, however, can be alternatively defined as family of all oriented planes being in oriented contact with two different cycles $\mathbf{c}_1, \mathbf{c}_2$. A cone of revolution thus has an isotropic circle $\Lambda(\mathbf{c}_1) \cap \Lambda(\mathbf{c}_2)$ as Λ -image. Note that the preimage of isotropic circles may degenerate to cylinders of revolution if the signed radii of \mathbf{c}_1 and \mathbf{c}_2 are equal, or to a pencil of planes in case of two nullcycles $\mathbf{c}_1, \mathbf{c}_2$.

We summarize: In the isotropic model of 3-dimensional Euclidean Laguerre space the oriented planes are represented by points of a 3-dimensional space I^3 . Oriented spheres (cycles) are mapped to isotropic Möbius spheres, i.e. paraboloids of revolution with isotropic axis or non-isotropic planes. Cones of revolution are represented by isotropic Möbius circles. Furthermore, Laguerre transformations (1) are realized as special quadratic transformations, so-called *isotropic Möbius transformations*. These are bijective on the set of Möbius spheres Σ .

2.2 Fundamentals on isotropic metric in I^3

The 3-dimensional isotropic space I^3 can be supplied with an isotropic metric that is derived from the semidefinite scalar product $\langle \rangle_i$ of two vectors $\mathbf{x}_1 = (x_1, y_1, z_1)$ and $\mathbf{x}_2 = (x_2, y_2, z_2)$

$$\langle \mathbf{x}_1, \mathbf{x}_2 \rangle_i = x_1 x_2 + y_1 y_2 \quad (8)$$

This defines the *isotropic distance* d_i of two points \mathbf{a}_1 and \mathbf{a}_2 by

$$d_i(\mathbf{a}_1, \mathbf{a}_2) := \sqrt{\langle \mathbf{a}_2 - \mathbf{a}_1, \mathbf{a}_2 - \mathbf{a}_1 \rangle_i} \quad (9)$$

Let $\tilde{\mathbf{a}} = (x_a, y_a)$ denote the normal projection of $\mathbf{a} = (x_a, y_a, z_a)$ into the xy -plane. Then (9) simply describes the Euclidean distance of $\tilde{\mathbf{a}}_1$ and $\tilde{\mathbf{a}}_2$. Consequently, the distance of two points lying on an isotropic line is zero.

Note that the isotropic distance is a metric property in I^3 (see e.g. [19]) and is not invariant under isotropic Möbius transformations.

In section 4 we will need the term *isotropic osculating circle* of a given twisted curve $g: \mathbf{g}(t) = (x(t), y(t), z(t))$ in I^3 . We may restrict ourselves to curves

which are regular and without inflection points and have no isotropic (z -parallel) tangents and isotropic osculating planes. Let $\tilde{\mathbf{g}}(t) = (x(t), y(t))$ again denote the top projection of g . To determine the isotropic osculating circle c of g at a point $\mathbf{g}(t_0)$ we intersect the cylinder of revolution through the osculating circle \tilde{c} of \tilde{g} at $\tilde{\mathbf{g}}(t_0)$ with the osculating plane in $\mathbf{g}(t_0)$, compare with Figure 2. Clearly, isotropic osculating circles are invariant under isotropic Möbius transformations.

3 Spatial isotropic biarc approximation of curves

We will briefly analyze the approximation of curves in I^3 with isotropic biarcs. Let \mathbf{a}_1 and \mathbf{a}_2 be two points of a given curve g and $\mathbf{p}_1, \mathbf{p}_2$ their tangent vectors which are normalized by $\langle \mathbf{p}_i, \mathbf{p}_i \rangle_i = 1$. The Hermite elements $(\mathbf{a}_i, \mathbf{p}_i), i = 1, 2$ shall now be connected by an isotropic biarc, i.e. a pair of isotropic arcs c_1 and c_2 joined with G^1 continuity.

Transforming this problem back from I^3 to the standard model of Euclidean Laguerre geometry with the map Λ^{-1} we obtain the approximation of a developable surface $\Lambda^{-1}(g)$ by a pair of cone segments $\Lambda^{-1}(c_1), \Lambda^{-1}(c_2)$. The Hermite data $(\mathbf{a}_i, \mathbf{p}_i)$ to be interpolated is the Λ image of the (oriented) Hermite elements (τ_i, e_i) , i.e. a set of planes τ_i each of which contains a ruling e_i .

Thus, approximation with isotropic biarcs is equivalent to the cone pair approximation introduced in [10]: From a developable surface take a sample of rulings and compute the tangent planes along these rulings. Then each two consecutive rulings plus tangent planes can be smoothly joined by a G^1 -pair of right circular cones. This results in a G^1 -cone spline surface.

But let us return to the isotropic biarcs. Completely analogous to the situation with Euclidean biarcs we define a control polygon for the Bézier representation of the isotropic biarc. The control points will be named by $\mathbf{a}_1, \mathbf{b}_1, \mathbf{c}, \mathbf{b}_2, \mathbf{a}_2$ (see Figure 2).

For $\mathbf{b}_1 = \mathbf{a}_1 + \lambda_1 \mathbf{p}_1$ and $\mathbf{b}_2 = \mathbf{a}_2 - \lambda_2 \mathbf{p}_2$ we obtain

$$\langle \mathbf{b}_2 - \mathbf{b}_1, \mathbf{b}_2 - \mathbf{b}_1 \rangle_i = (\lambda_1 + \lambda_2)^2, \quad (10)$$

as the normal projections \tilde{c}_1, \tilde{c}_2 of the isotropic arcs c_1, c_2 have to be Euclidean circles. There is a one parameter set of solutions which we can get by choosing $\mathbf{b}_1(\lambda_1)$ and computing $\mathbf{b}_2(\lambda_2)$ via (10). The junction point \mathbf{c} can be computed by

$$\mathbf{c} = \frac{\lambda_2 \mathbf{b}_1 + \lambda_1 \mathbf{b}_2}{\lambda_1 + \lambda_2}.$$

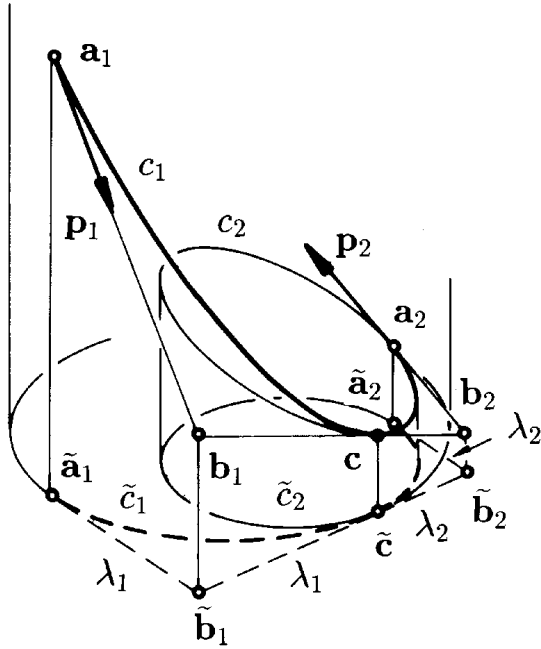


Figure 2: Isotropic biarcs

For the representation of c_i as rational Bézier curves of degree two (see e.g. [5]) we have weights 1 at \mathbf{a}_i and \mathbf{c} and weights w_i at \mathbf{b}_i which satisfy

$$|w_i| = \frac{|\langle \mathbf{b}_i - \mathbf{a}_i, \mathbf{c} - \mathbf{a}_i \rangle_i|}{d_i(\mathbf{a}_i, \mathbf{b}_i)d_i(\mathbf{a}_i, \mathbf{c})}.$$

The sign of w_1 and w_2 has to be chosen equal to the sign of λ_1 and λ_2 . Positive values of λ_i indicate that the arc contained in the triangle $\mathbf{a}_i, \mathbf{b}_i, \mathbf{c}$ is used, thus a positive weight w_i is needed.

In Euclidean 3-space we know [10]

Theorem 3.1 *Given two G^1 elements $(e_1, \tau_1), (e_2, \tau_2)$, i.e. rulings plus tangent planes, in general position, there is a one parameter family of cone pairs interpolating this data. The cones possess a common inscribed sphere Σ . The tangent planes at the junction generators of the cone pairs, as well as the planes τ_1 and τ_2 , touch Σ along a circle.*

Transferring this result via the map $\Lambda : \mathbf{U} \rightarrow I^3$ we obtain

Theorem 3.2 *Given two G^1 -elements $(\mathbf{a}_1, \mathbf{p}_1), (\mathbf{a}_2, \mathbf{p}_2)$ in general position, there is a one parameter family of isotropic biarcs c_1, c_2 interpolating this data. The isotropic circles c_i all lie on an isotropic sphere Σ which is uniquely determined by $(\mathbf{a}_i, \mathbf{p}_i)$. The junction point \mathbf{c} varies on an isotropic circle c which lies on Σ and passes through \mathbf{a}_1 and \mathbf{a}_2 .*

Note that Theorem 3.2 is an analogue to the identical one in Euclidean 3-space (see e.g. [6, 20]).

4 Spatial isotropic osculating arc splines

Let \mathbf{a}_1 and \mathbf{a}_2 be two points of a given curve g in I^3 which is regular and has no isotropic tangents. The oriented isotropic circles c_1 and c_2 osculating g in \mathbf{a}_1 and \mathbf{a}_2 lie in the planes σ_1 and σ_2 . Our aim is to find an isotropic circle c joining c_1 and c_2 with G^1 continuity in the junction points \mathbf{c}_1 and \mathbf{c}_2 (see Figure 3). With

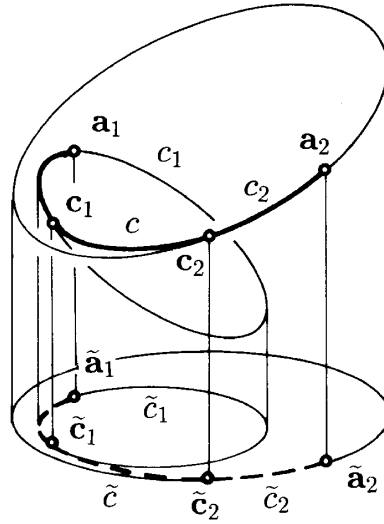


Figure 3: Isotropic osculating arcs

this method we are able to construct an isotropic arc spline approximating g so that every second arc is an isotropic osculating circle of g in a point \mathbf{a}_i . Although we use three arcs to join the two points $\mathbf{a}_1, \mathbf{a}_2$ the method produces an arc spline with about the same number of arcs as the biarc method does. This is because the next segment between \mathbf{a}_2 and \mathbf{a}_3 is continued with the isotropic arc c_2 .

The investigation of isotropic osculating arc splines is motivated by the fact that it is the Λ -image of the osculating cone spline approximation scheme in [10]: From a given developable surface $\Gamma = \Lambda^{-1}(g)$ we choose certain generators to oriented tangent planes $\tau_i = \Lambda^{-1}(\mathbf{a}_i)$ and join two consecutive oriented osculating cones $\Delta_i = \Lambda^{-1}(c_i)$ by a cone segment $\Delta = \Lambda^{-1}(c)$. Thus, every second of the circular cone patches of the resulting G^1 -cone spline surface is an osculating cone of the target surface Γ .

As curves are easier to handle than surfaces it is often preferable to work with isotropic circles in I^3 than with cones of revolution in E^3 . Therefore, in section 4.1 we will first analyze geometrically how to find an isotropic arc c

joining two isotropic circles c_1, c_2 which are osculating a curve g to parameter values t_1, t_2 . In general we obtain two solutions for c which need not be real. In section 4.2 we will be able to prove, however, that there is a real and useful solution arc c if the difference between the parameter values t_i is sufficiently small. In our proof we will simplify the geometric situation by applying an appropriate isotropic Möbius transformation $\alpha : I^3 \rightarrow I^3$.

4.1 Method

The normal projection of c_1, c, c_2 into the xy -plane is an (Euclidean) arc spline $\tilde{c}_1, \tilde{c}, \tilde{c}_2$ which we will examine first. Note that the pre-images $\mathbf{u} = \Lambda^{-1}(\mathbf{x})$ and $\tilde{\mathbf{u}} = \Lambda^{-1}(\tilde{\mathbf{x}})$ of a point $\mathbf{x} \in I^3$ and its top projection $\tilde{\mathbf{x}}$ are parallel planes and $\tilde{\mathbf{u}}$ contains the origin $\mathbf{o} \in E^3$. The top view of the isotropic triarc c_1, c, c_2 therefore is equivalent to a translation of the cones $\Lambda^{-1}(\mathbf{c}), \Lambda^{-1}(\mathbf{c}_i)$ so that they possess the common vertex \mathbf{o} .

It is well known that there is a one parameter set of circles c being in oriented contact with \tilde{c}_1, \tilde{c}_2 (see for instance [14]). Quite recently the approximation quality of planar osculating arc splines has been analyzed in [13].

We will define a control polygon for the arc spline and denote its points by $\tilde{\mathbf{a}}_1, \dots, \tilde{\mathbf{a}}_2$ (see Figure 4). After choosing the first junction point $\tilde{\mathbf{c}}_1(\lambda_1)$, where λ_1

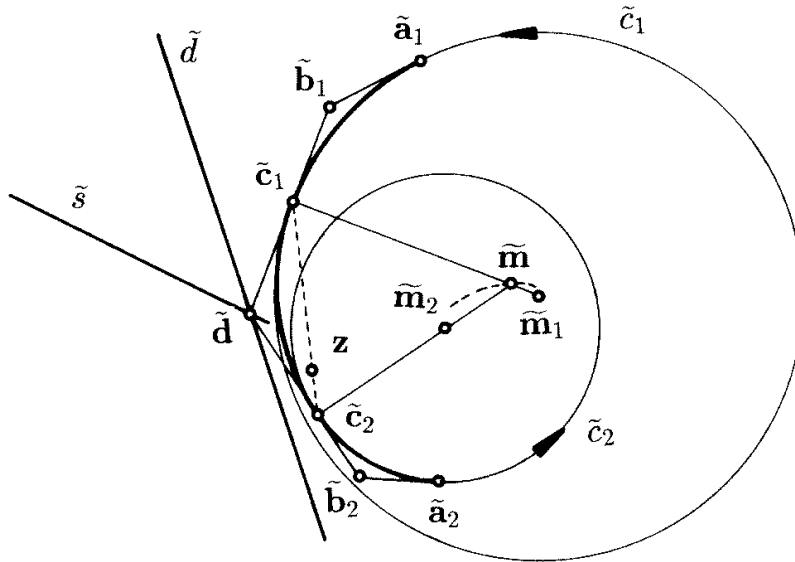


Figure 4: Planar Euclidean osculating arcs

is a homogeneous parameter on the oriented circle c_1 , the second junction point $\tilde{\mathbf{c}}_2(\lambda_2)$ is uniquely determined. $\tilde{\mathbf{c}}_1(\lambda_1) \mapsto \tilde{\mathbf{c}}_2(\lambda_2)$ is a projective mapping. It is an important property that the middle control point $\tilde{\mathbf{d}}$ of \tilde{c} has to lie on the chordal

line \tilde{d} of the two circles \tilde{c}_1, \tilde{c}_2 since \tilde{d} contains all points whose tangential distances to \tilde{c}_1 and \tilde{c}_2 are equal. The equation of \tilde{d} in affine coordinates is

$$\tilde{d}: 2\mathbf{x}(\tilde{\mathbf{m}}_2 - \tilde{\mathbf{m}}_1) - (r_1^2 - r_2^2) + (\tilde{\mathbf{m}}_1^2 + \tilde{\mathbf{m}}_2^2) = 0 \quad (11)$$

where r_i denote the radii and $\tilde{\mathbf{m}}_i$ the midpoints of \tilde{c}_i . For the implementation of the projective map $\tilde{\mathbf{c}}_1(\lambda_1) \mapsto \tilde{\mathbf{c}}_2(\lambda_2)$ it is helpful to be aware of the fact that the connecting lines of matching points $\tilde{\mathbf{c}}_1$ and $\tilde{\mathbf{c}}_2$ always pass through a point \mathbf{z} . This property can be verified as follows: Let \varkappa_1 equal the homothety with center \mathbf{z} and $\varkappa_1(\tilde{c}_1) = \tilde{c}_2$, preserving the orientation of \tilde{c}_i . \mathbf{z} is given by

$$\mathbf{z} = \frac{r_2}{r_2 - r_1} \tilde{\mathbf{m}}_1 - \frac{r_1}{r_2 - r_1} \tilde{\mathbf{m}}_2 \quad (12)$$

where the radii r_i of \tilde{c}_i are oriented. Denote the \tilde{c}_2 -automorphic harmonic perspectivity with center \mathbf{z} by \varkappa_2 . Then the composition $\varkappa = \varkappa_1 \varkappa_2$ is a perspective collineation with center \mathbf{z} and axis \tilde{d} because the points of $\tilde{c}_1 \cap \tilde{c}_2$ are fixed under \varkappa . Now the restriction of \varkappa to \tilde{c}_1 gives the projective map $\mathbf{c}_1(\lambda_1) \mapsto \mathbf{c}_2(\lambda_2)$.

Furthermore, the midpoints $\tilde{\mathbf{m}}$ of the one parameter family of joining arcs lie on a conic with focal points $\tilde{\mathbf{m}}_1$ and $\tilde{\mathbf{m}}_2$ which directly follows from the basic definition of conics. Another way to realize the projective map $\tilde{\mathbf{c}}_1 \mapsto \tilde{\mathbf{c}}_2$ is to choose $\tilde{\mathbf{c}}_1$ and thus finding $\tilde{\mathbf{d}}$ by intersecting the tangent in $\tilde{\mathbf{c}}_1$ with \tilde{d} . Laying a tangent from $\tilde{\mathbf{d}}$ to \tilde{c}_2 one gets $\tilde{\mathbf{c}}_2$ which is unique because both circles \tilde{c}_i are oriented.

We will now return to the spatial problem in I^3 : a possible solution arc \tilde{c} with junction points $\tilde{\mathbf{c}}_i$ of the planar problem does not necessarily lead to a solution arc c of the spatial problem because the tangents t_i in \mathbf{c}_i to c_i generally lie in different osculating planes σ_1 and σ_2 and need not have a point \mathbf{d} in common. As this point \mathbf{d} cannot but lie on the intersection line $s = \sigma_1 \sigma_2$ it is necessary for $\tilde{\mathbf{d}}$ to lie on both \tilde{d} and the top projection \tilde{s} of s . If $\tilde{\mathbf{d}}$ lies outside of \tilde{c}_1 and \tilde{c}_2 one gets two real solution arcs c . One just has to lay both tangents out of $\tilde{\mathbf{d}}$ to \tilde{c}_i and thus determine the junction points while taking care of the circles' orientation.

In the special cases of $\sigma_1 = \sigma_2$ and $\tilde{s} = \tilde{d}$ there is a one parameter set of isotropic solution arcs c joining c_1 and c_2 . This happens exactly if c_1 and c_2 lie on a common isotropic Möbius sphere, i.e. a non-isotropic plane or a paraboloid of revolution. Reinterpreting with Λ^{-1} , we confirm the existence of a one parameter set of cones Δ in oriented contact with two given cones of revolution Δ_1, Δ_2 if both Δ_i are in oriented contact with a common sphere Σ . This includes the case of Δ_i possessing the same vertex \mathbf{v} since the common vertex can be interpreted as sphere with radius zero.

4.2 Feasibility of the solution

In order to show the reality and usefulness of a solution arc c we will prove

Theorem 4.1 *Let $\mathbf{g}(t)$ be a piecewise C^∞ curve in isotropic 3-space I^3 . To any point $\mathbf{g}(t_1)$ there exists a parameter interval $U =]t_1, t_1 + \Delta t] \subset \mathbb{R}$ such that the points $\mathbf{g}(t_1)$ and $\mathbf{g}(t_2), t_2 \in U$ can be joined with an isotropic triarc in the following way: the first and the third arc of this triarc lie on the isotropic osculating circles c_1 and c_2 of $\mathbf{g}(t)$ to parameters t_1 and t_2 . The joining isotropic arc c is real and joins c_1 and c_2 with G^1 -continuity while preserving the orientation of c_i .*

Via the transition of the isotropic model into the standard model of Euclidean Laguerre geometry Theorem 4.1 is equivalent to

Theorem 4.2 *Let Γ be a piecewise C^∞ developable surface. To any osculating cone $\Delta(t_1)$ of Γ to parameter t_1 , there exists a parameter interval $U =]t_1, t_1 + \Delta t] \subset \mathbb{R}$ such that the osculating cones $\Delta(t_1)$ and $\Delta(t_2), t_2 \in U$ can be smoothly joined with a cone Δ . The joining cone Δ is real and joins Δ_1 and Δ_2 with G^1 -continuity while preserving the orientation of Δ_i .*

Proof: (of Theorem 4.1)

We apply an isotropic Möbius transformation $\alpha : I^3 \rightarrow I^3$ to the curve g such that the first isotropic osculating circle c_1 is mapped to the x -axis. As the order of contact between g and c_1 is not changed by α the x -axis is an inflection tangent to $\alpha(g)$.

Without loss of generality we can restrict ourselves to a curve $g = \mathbf{g}(t)$ which has an inflection point $\mathbf{g}(0)$ to parameter $t = 0$ at the origin \mathbf{o} . Let its inflection tangent be the x -axis and $\mathbf{g}(0) + \lambda_1 \dot{\mathbf{g}}(0) + \lambda_2 \mathbf{g}^{(3)}(0)$ be the xy -plane. A Taylor expansion of $\mathbf{g}(t)$ up to the fourth derivative is then given by

$$\mathbf{g}(t) = \begin{pmatrix} a_1 t + a_2 t^2 + a_3 t^3 + a_4 t^4 + O(t^5) \\ b_3 t^3 + b_4 t^4 + O(t^5) \\ c_4 t^4 + O(t^5) \end{pmatrix}, a_1, b_3, c_4 \in \mathbb{R}^+; a_i, b_i, c_i \in \mathbb{R} \quad (13)$$

with derivatives

$$\dot{\mathbf{g}}(t) = \begin{pmatrix} a_1 + 2a_2 t + 3a_3 t^2 + 4a_4 t^3 + O(t^4) \\ 3b_3 t^2 + 4b_4 t^3 + O(t^4) \\ 4c_4 t^3 + O(t^4) \end{pmatrix} \quad (14)$$

and

$$\ddot{\mathbf{g}}(t) = \begin{pmatrix} 2a_2 + 6a_3 t + 12a_4 t^2 + O(t^3) \\ 6b_3 t + 12b_4 t^2 + O(t^3) \\ 12c_4 t^2 + O(t^3) \end{pmatrix}. \quad (15)$$

We will compute the control points $\mathbf{c}_1, \mathbf{d}, \mathbf{c}_2$ of an isotropic arc c which is in oriented contact with the x -axis and the isotropic circle $c_2(t)$ which osculates g in $\mathbf{g}(t)$ (see Figure 5, where the connecting arc c has been omitted as it lies too close to the curve g). The middle control point \mathbf{d} is the intersection point of

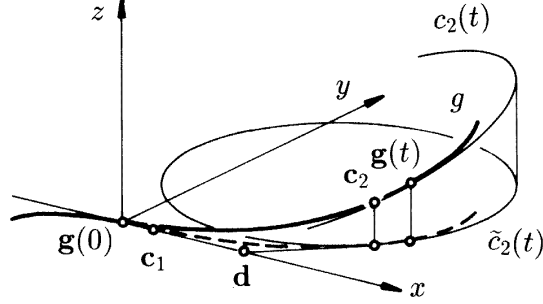


Figure 5: $\mathbf{g}(t)$ with inflection point $\mathbf{g}(0)$

the osculating plane σ_2 at $\mathbf{g}(t)$ with the x -axis. The junction point \mathbf{c}_2 can be computed by laying a tangent from \mathbf{d} to $c_2(t)$. The last control point \mathbf{c}_1 on the x -axis is determined by

$$d_i(\mathbf{c}_1, \mathbf{d}) = d_i(\mathbf{c}_2, \mathbf{d}). \quad (16)$$

We will now calculate $\mathbf{c}_1, \mathbf{d}, \mathbf{c}_2$ in dependency on t and will show that for $t \rightarrow 0$, i.e. the touching point $\mathbf{g}(t)$ to $c_2(t)$ converges to $\mathbf{g}(0)$, we will obtain a useful arc c .

Defining the normal vector

$$\mathbf{n}(t) = \dot{\mathbf{g}}(t) \times \ddot{\mathbf{g}}(t) = \begin{pmatrix} 12c_4b_3t^4 + O(t^5) \\ -12a_1c_4t^2 + O(t^3) \\ 6a_1b_3t + 6(2a_1b_4 + a_2b_3)t^2 + O(t^3) \end{pmatrix} \quad (17)$$

of $\sigma_2(t)$, one gets

$$\sigma_2(t) : \mathbf{n}(t) \cdot \mathbf{x} = \mathbf{n}(t) \cdot \mathbf{g}(t)$$

and easily verifies

$$\mathbf{d}(t) = \sigma_2(t) \cap x\text{-axis} = \begin{pmatrix} \frac{1}{2}a_1t + O(t^2) \\ 0 \\ 0 \end{pmatrix}. \quad (18)$$

The following calculations will be made for the top projection \tilde{g} of g . The top view of $c_2(t)$ is the (Euclidean) osculating circle $\tilde{c}_2(t)$ of \tilde{g} at $\tilde{\mathbf{g}}(t)$. Its radius equals

$$\tilde{r} = \frac{\|\dot{\tilde{\mathbf{g}}}\|^3}{\det \begin{pmatrix} \dot{\tilde{\mathbf{g}}} \\ \ddot{\tilde{\mathbf{g}}} \end{pmatrix}}.$$

Formulae (14) and (15) give

$$\tilde{r}^2(t) = \frac{1}{t^2} \left(\frac{a_1^4}{36b_3^2} + \frac{5a_1^3a_2b_3 - 2a_1^4b_4}{18b_3^2}t + O(t^2) \right). \quad (19)$$

The midpoint $\tilde{\mathbf{m}}(t)$ of $\tilde{c}_2(t)$

$$\tilde{\mathbf{m}}(t) = \tilde{\mathbf{g}}(t) + \frac{\|\dot{\tilde{\mathbf{g}}}(t)\|^2}{\det(\dot{\tilde{\mathbf{g}}}(t), \ddot{\tilde{\mathbf{g}}}(t))} \cdot \dot{\tilde{\mathbf{g}}}^\perp(t)$$

simplifies to

$$\tilde{\mathbf{m}}(t) = \left(\begin{array}{c} \frac{1}{2}a_1t + O(t^2) \\ \frac{1}{t} \left(\frac{a_1^2}{6b_3} + \frac{5a_1a_2b_3 - 2a_1^2b_4}{6b_3^2}t + O(t^2) \right) \end{array} \right). \quad (20)$$

The square of the distance $\tilde{R}(t)$ between $\mathbf{d}(t)$ and $\tilde{\mathbf{m}}(t)$ equals

$$\tilde{R}^2(t) = (\tilde{\mathbf{m}}(t) - \mathbf{d}(t))^2 = \frac{1}{t^2} \left(\frac{a_1^4}{36b_3^2} + \frac{5a_1^3a_2b_3 - 2a_1^4b_4}{18b_3^2}t + O(t^2) \right). \quad (21)$$

Using coefficients of higher order in t , which have been omitted in formulae (19) and (21), one verifies for the power $\tilde{p}(t)$ of the point $\mathbf{d}(t)$ with respect to the circle $\tilde{c}_2(t)$

$$\tilde{p}(t) = \tilde{R}^2(t) - \tilde{r}^2(t) = \frac{1}{12}a_1^2t^2 + O(t^3). \quad (22)$$

The value of $\tilde{p}(t)$ is positive if t is sufficiently small. Thus, $\mathbf{d}(t)$ lies outside of $\tilde{c}_2(t)$ and $\tilde{c}_2(t)$ and $\mathbf{c}_2(t)$ are real.

The power $\tilde{p}(t)$ is the square of the distance of $\mathbf{d}(t)$ and $\tilde{c}_2(t)$ and together with (16) we have

$$\tilde{p}(t) = (\mathbf{d}(t) - \tilde{\mathbf{c}}_2(t))^2 = (\mathbf{d}(t) - \tilde{\mathbf{c}}_1(t))^2.$$

(18) and (13) show that the squares of the distances of $\mathbf{d}(t)$ to $\mathbf{o} = \tilde{\mathbf{g}}(0)$ and $\tilde{\mathbf{g}}(t)$ simplify to

$$(\mathbf{d}(t) - \tilde{\mathbf{g}}(0))^2 = (\mathbf{d}(t) - \tilde{\mathbf{g}}(t))^2 = \frac{1}{4}a_1^2t^2 + O(t^3) \quad (23)$$

which is greater than $\tilde{p}(t)$ in formula (22). This shows that for small t the x -coordinate of $\mathbf{c}_1(t)$ is positive and the x -coordinate of $\mathbf{c}_2(t)$ is smaller than the x -coordinate of $\mathbf{g}(t)$ (see Figure 5). \square

5 Spatial Euclidean Arc Splines

In 3-dimensional Euclidean space E^3 the approximation of twisted curves with *spatial (Euclidean) biarcs* is well understood (see e.g. [6, 8, 15, 20]). Approximation schemes with osculating arc splines have been analyzed for the planar Euclidean case [13], and recently also for the 3-dimensional Euclidean case [12].

Figure 6 (a) shows the approximation of a helical curve (thin curve) by one triarc segment (thick curve) in top view and front view. Figure 6 (b) shows the approximation of the same curve with two triarc segments. The big octahedrons

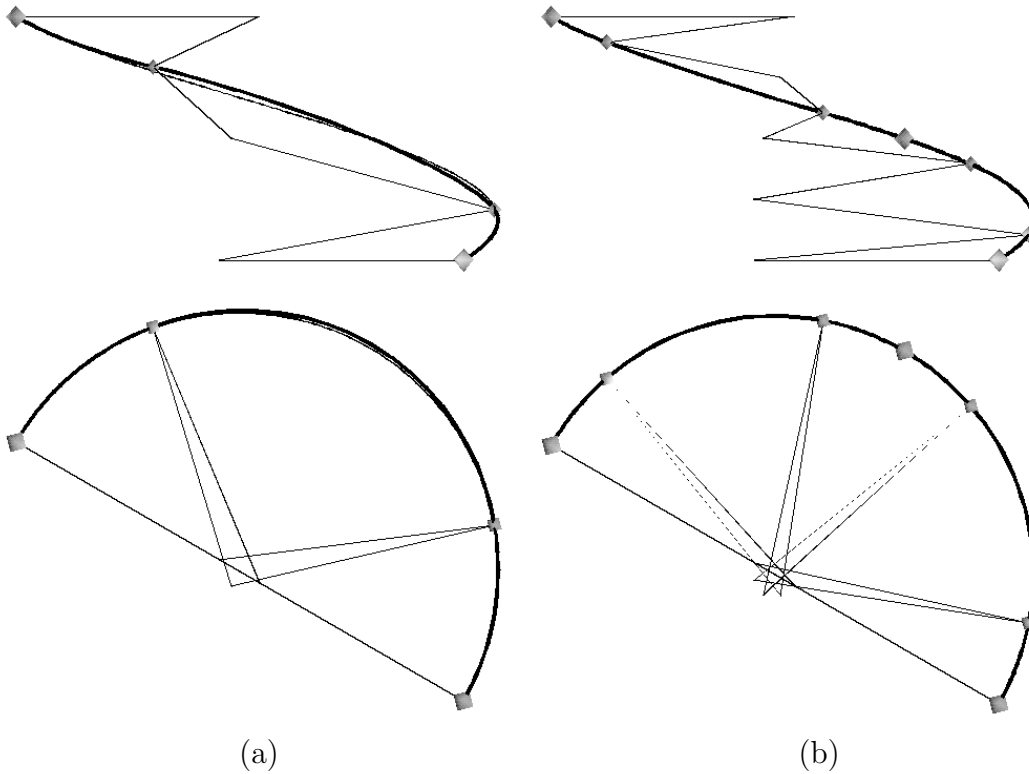


Figure 6: Approximation with (a) one, (b) two triarc segments

indicate the curve points whose osculating circles were computed. The smaller octahedron are the joining points of different arc segments. In order to better illustrate the spatial position of the arc segments their end points are connected to their midpoint with thin lines. For further information of approximation errors and practical segmentation algorithms of the given curve the reader is referred to [12].

It is natural to introduce 3-dimensional Euclidean Möbius geometry in section 5.1 since the set of Euclidean Möbius circles is comprised of straight lines and Euclidean circles. Speaking of a G^1 circular arc spline one tacitly allows degeneration of circular arc segments to straight line segments.

Similar to section 4.2 we will use a Möbius transformation in order to simplify the proof of Theorem 5.1 in section 5.2: two osculating circles c_1, c_2 of a curve g can be joined by a real and useful arc c as long as the difference of parameters t_1, t_2 associated with c_1, c_2 is small enough.

5.1 3-dimensional Euclidean Möbius geometry

Let E^3 be real Euclidean 3-space, P its point set and M the set of spheres and planes of E^3 . We obtain the so-called *Euclidean conformal closure* E_M^3 of E^3 by extending the point set P by an arbitrary element $\mathbf{x}_u \notin P$ to $P_M = P \cup \{\mathbf{x}_u\}$. As an extension of the incidence relation we define that \mathbf{x}_u lies in all planes but in none of the spheres. The elements of M are called *Euclidean Möbius spheres* and the intersection of two Möbius spheres is a so-called *Euclidean Möbius circle*. Euclidean Möbius geometry is the study of properties that are invariant under *Euclidean Möbius transformations*. A Möbius transformation is an incidence preserving composition of a bijective map of P_M and a bijective map of M .

Another model of this geometry we obtain by embedding E^3 in Euclidean 4-space E^4 as plane $t = 0$. Let $\sigma : \Sigma \setminus \{\mathbf{z}\} \rightarrow E^3$ be the stereographic projection of the unit hypersphere

$$\Sigma : x^2 + y^2 + z^2 + t^2 = 1 \quad (24)$$

onto E^3 with center $\mathbf{z} = (0, 0, 0, 1)$. Extending σ to $\bar{\sigma}$ with $\bar{\sigma} : \mathbf{z} \mapsto \mathbf{x}_u$ gives a new model of Euclidean Möbius geometry. The point set is that of $\Sigma \subset E^4$ and the Möbius spheres are the hyperplanar intersections of Σ since σ is preserving spheres. It is a central theorem of Euclidean Möbius geometry that all Euclidean Möbius transformations of this model are induced by an automorphic linear map $P^4 \rightarrow P^4$ of Σ , where P^4 denotes the projective extension of E^4 .

5.2 Feasibility of the solution

Completely analogous to the isotropic case in 4.2 we state

Theorem 5.1 *Let $\mathbf{g}(t)$ be a piecewise C^∞ curve in Euclidean 3-space E^3 . To any point $\mathbf{g}(t_1)$ there exists a parameter interval $U =]t_1, t_1 + \Delta t] \subset \mathbb{R}$ such that the points $\mathbf{g}(t_1)$ and $\mathbf{g}(t_2), t_2 \in U$ can be joined with a Euclidean triarc in the following way: the first and the third arc of this triarc lie on the Euclidean osculating circles c_1 and c_2 of $\mathbf{g}(t)$ to parameters t_1 and t_2 . The joining Euclidean arc c is real and joins c_1 and c_2 with G^1 -continuity while preserving the orientation of c_i .*

Proof: We apply a Euclidean Möbius transformation to the curve g such that the first osculating circle c_1 is mapped to the x -axis. Thus, we can restrict our calculations to curves $g = \mathbf{g}(t)$ with an inflection point at $\mathbf{g}(0) = \mathbf{o}$.

We will compute the control points $\mathbf{c}_1, \mathbf{d}, \mathbf{c}_2$ of an arc c which is in oriented contact with the x -axis and the osculating circle c_2 of g to parameter t . The middle control point \mathbf{d} can be found as intersection point of the osculating plane σ_2 with the x -axis (Figure 7). The junction point \mathbf{c}_2 can be determined by laying

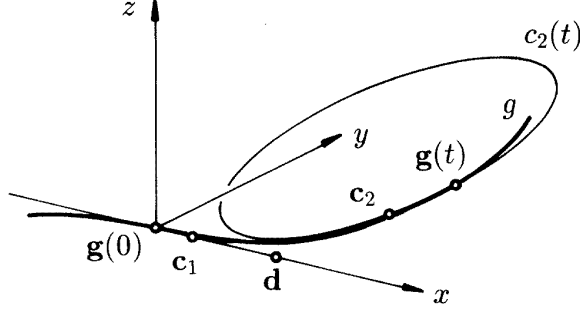


Figure 7: $\mathbf{g}(t)$ with inflection point $\mathbf{g}(0)$

a tangent from \mathbf{d} to c_2 and \mathbf{c}_1 follows from

$$\|\mathbf{c}_1 - \mathbf{d}\| = \|\mathbf{c}_2 - \mathbf{d}\|. \quad (25)$$

The only difference to section 4.2 is that c_2 is a Euclidean circle and the distances in (25) are Euclidean ones.

We can use (13) to (15), (17) and (18) for the Taylor expansions of $\mathbf{g}(t), \dot{\mathbf{g}}(t), \ddot{\mathbf{g}}(t), \mathbf{n}(t)$ and $\mathbf{d}(t)$. The radius $r(t)$ of the (Euclidean) osculating circle $c_2(t)$ of g at $\mathbf{g}(t)$ equals

$$r = \frac{\|\dot{\mathbf{g}}\|^3}{\|\mathbf{n}(t)\|}$$

and with (14) and (17) simplifies to

$$r^2(t) = \frac{1}{t^2} \left(\frac{a_1^4}{36b_3^2} + \frac{5a_1^3a_2b_3 - 2a_1^4b_4}{18b_3^2}t + O(t^2) \right). \quad (26)$$

The midpoint $\mathbf{m}(t)$ of $c_2(t)$

$$\mathbf{m}(t) = \mathbf{g}(t) + \frac{\|\dot{\mathbf{g}}(t)\|^2}{\|\mathbf{n}(t)\|^2} \cdot (\mathbf{n}(t) \times \dot{\mathbf{g}}(t))$$

possesses Taylor expansions

$$\mathbf{m}(t) = \begin{pmatrix} \frac{1}{t} \left(\frac{a_1^2}{6b_3} + \frac{\frac{1}{2}a_1t + O(t^2)}{6b_3^2} \right) \\ \frac{a_1^2c_4}{3b_3^2} + O(t) \end{pmatrix}. \quad (27)$$

The square of the distance $R(t)$ between $\mathbf{d}(t)$ and $\mathbf{m}(t)$ equals

$$R^2(t) = (\mathbf{m}(t) - \mathbf{d}(t))^2 = \frac{1}{t^2} \left(\frac{a_1^4}{36b_3^2} + \frac{5a_1^3a_2b_3 - 2a_1^4b_4}{18b_3^2}t + O(t^2) \right) \quad (28)$$

which, similar to the proof of Theorem 4.1, leads to

$$p(t) = R^2(t) - r^2(t) = \frac{1}{12}a_1^2t^2 + O(t^3)$$

for the power of $\mathbf{d}(t)$ with respect to c_2 . If t is small enough the value of $p(t)$ is positive but smaller than

$$(\mathbf{d}(t) - \mathbf{g}(0))^2 = (\mathbf{d}(t) - \mathbf{g}(t))^2 = \frac{1}{4}a_1^2t^2 + O(t^3).$$

Therefore, a real and useful solution arc c exists which provides a triarc connection of $\mathbf{g}(0)$ and $\mathbf{g}(t)$. \square

6 Summary and future research

Classical sphere geometric models can be used to provide a point representation of (oriented) planes, thus a curve representation of developable surfaces. Most importantly, cones of revolution are mapped to circles with respect to an isotropic metric in a 3-dimensional space.

A topic for future research are other Hermite-like approximation schemes of developable surfaces with cone spline surfaces. One might, for example, interpolate two tangent planes plus rulings and points of regression $(\tau_i, e_i, \mathbf{v}_i)$ with three cone segments. There is a two-parameter set of solutions for this triple: One can choose the first circular cone patch Λ_1 with vertex \mathbf{v}_1 such that it touches tangent plane τ_1 along e_1 and do the same for the third cone patch Λ_3 . Then, there are two complex circular cone patches Λ_2 that smoothly join Λ_1 and Λ_3 (see section 4).

Appropriate selection algorithms for the free parameters and theorems on the existence of real joining cones Λ_2 should be easier to derive, as one makes use of the isotropic model of Euclidean Laguerre geometry as described in this paper.

Acknowledgements

This work has been supported in part by grant No. P12252-MAT of the Austrian Science Foundation.

References

- [1] W. Benz, *Geometrische Transformationen* (BI-Wiss.-Verlag, Mannheim, 1992).
- [2] W. Blaschke, *Vorlesungen über Differentialgeometrie III* (Springer, Berlin, 1929).
- [3] T.E. Cecil, *Lie Sphere Geometry* (Springer-Verlag, New York, 1992).
- [4] J.C. Clements and L.J. Leon, A fast accurate algorithm for the isometric mapping of a developable surface, *SIAM J. Math. Anal.* 18(1987)966–971.
- [5] G. Farin, *Curves and Surfaces for Computer Aided Geometric Design* (Academic Press, Boston, 3rd edn., 1992).
- [6] W. Fuhs and H. Stachel, Circular pipe connections, *Computers & Graphics* 12(1988)53–57.
- [7] B. Gurunathan and S.G. Dhande, Algorithms for development of certain classes of ruled surfaces, *Computers & Graphics* 11(1987)105–112.
- [8] J. Hoschek, Circular splines, *Computer-Aided Design* 24(1992)611–618.
- [9] E. Kreyszig, A new standard isometry of developable surfaces in CAD/CAM, *SIAM J. Math. Anal.* 25(1994)174–178.
- [10] S. Leopoldseder and H. Pottmann, Approximation of developable surfaces with cone spline surfaces, *Computer-Aided Design* 30(1998)571–582.
- [11] S. Leopoldseder, Cone spline surfaces and spatial arc splines, Dissertation, TU Wien (1998).
- [12] S. Leopoldseder, Algorithms on cone spline surfaces and spatial osculating arc splines, Technical report 76, Institut für Geometrie, TU Wien (2000).
- [13] D.S. Meek and D.J. Walton, Planar osculating arc splines, *Computer Aided Geometric Design* 13(1996)653–671.
- [14] E. Müller, *Vorlesungen über Darstellende Geometrie, II. Band: Die Zyklographie*, herausgegeben von J.L. Krames (Franz Deuticke, Wien, 1929).
- [15] A.W. Nutbourne and R.R. Martin, *Differential Geometry Applied to Curve and Surface Design. Vol. 1: Foundations* (Ellis Horwood, 1988).
- [16] M. Peternell and H. Pottmann, A Laguerre Geometric Approach to Rational Offsets, *Computer Aided Geometric Design* 15(1998)223–249.
- [17] H. Pottmann and M. Peternell, Applications of Laguerre geometry in CAGD, *Computer Aided Geometric Design* 15(1998)165–186.
- [18] P. Redont, Representation and deformation of developable surfaces, *Computer-Aided Design* 21(1989)13–20.

- [19] H. Sachs, *Isotrope Geometrie des Raumes* (Vieweg, Braunschweig, 1990).
- [20] T.J. Sharrock, Biarcs in three dimensions, in: *Mathematics of Surfaces II*, ed. R.R. Martin (Oxford University Press, 1986).
- [21] G. Weiss and P. Furtner, Computer-aided treatment of developable surfaces, *Computers & Graphics* 12(1988)39–51.